BMC Plant Biology

RESEARCH

Open Access

Insights into membrane-bound fatty acid desaturase genes in tigernut (*Cyperus esculentus* L.), an oil-rich tuber plant in Cyperaceae

Zhi Zou[1*], Xiaowen Fu[1], Chunqiang Li[1], Jiaquan Huang[1,2*] and Yongguo Zhao[1,3*]

Abstract

Background Tigernut (*Cyperus esculentus* L.), an oil-rich tuber plant of the Cyperaceae family, is typical for the naturally high content of oleic acid. However, to date, genes contributing to oil composition have not been well characterized.

Results In this study, the first genome-wide analysis of tigernut genes encoding membrane-bound fatty acid desaturases (FADs), the key contributors to oil composition, is presented. According to phylogenetic analysis, ten members identified from the tigernut genome were assigned into seven out of eight evolutionary groups as defined in *Arabidopsis thaliana*, i.e., FAD2 (3), FAD6 (1), FAD3 (1), FAD7 (1), FAD4 (1), DES (1), and SLD (2). In contrast to the absence of an FAD5 homolog, FAD2 and SLD in tigernut were shown to have expanded via tandem and dispersed duplications, respectively. Comparison of 285 members from 29 representative plant species resulted in 11 orthogroups, where FAD2a, FAD6, FAD7, FAD3, FAD4, FAD5, DES, and SLD1 were shown to have already appeared in the ancestor of seed plants. Significantly, orthologous and syntenic analyses revealed that loss of FAD5 and expansion of SLD in tigernut are lineage-specific, occurred sometime before the radiation of core monocots, in contrast to species-specific expansion of FAD2. Moreover, though no syntenic relationship was observed between *CeFAD* genes, our comparative genomics analyses indicated that FAD3 and -7 are more likely to arise from segmental duplication. Structural variation and expression divergence of *CeFAD* genes were also observed. Gain of introns in *CeFAD4*, *CeSLD1*, and *CeSLD2* was shown to be lineage-specific, occurred sometime before Cyperaceae-Juncaceae split. Tissue-specific expression analysis revealed that *CeFAD2-1*, *CeFAD6*, and *CeFAD7* were constitutively expressed, whereas others were tissue-specific. Among five paralogs identified, *CeFAD2-1* and *CeSLD1* have evolved to be two dominant members. Putative roles of *CeFAD2-1* in oil accumulation are supported by 1) exhibited an expression pattern positively associated with oil accumulation during tuber development; 2) were expressed more in tubers than their orthologs in *C. rotundus*. Additionally, in contrast to high expression of *CrFAD3*, transcript levels of *CeFAD3* in tubers were fairly low, which may explain the distinct α-linolenic acid content between these two close species.

*Correspondence:
Zhi Zou
zouzhi2008@126.com
Jiaquan Huang
jqhuang@hainanu.edu.cn
Yongguo Zhao
zhaoyongguo@gdupt.edu.cn
Full list of author information is available at the end of the article

Conclusions Our findings provide a global view of *CeFAD* genes, which not only highlights lineage-specific evolution of the family, but also provides valuable information for further functional analysis and genetic improvement in tigernut.

Keywords *Cyperus esculentus*, Vegetative tissue, Underground tuber, FAD, Phylogenomics, Orthologous analysis, Syntenic analysis

Background

Fatty acids (FAs) are key cell components that are involved in various plant physiological processes. According to the presence or absence of double bonds, FAs are classified into saturated and unsaturated FAs, where the latter could be further divided into monounsaturated FAs (MUFAs) and polyunsaturated FAs (PUFAs) [1]. The desaturation reaction of FAs is catalyzed by a class of enzymes known as FA desaturases (FADs), which could insert double bonds into the fatty acyl chain. There are two main categories of FADs present in plants, i.e., soluble and membrane-bound, which share no significant sequence similarity [2]. Soluble FADs are located in the stroma of plastids and could introduce a double-bond at the Δ9 position of FA bounded to acyl carrier protein (ACP), which possess two main types with substrate selectivity toward stearic acid (SA, 18:0) and palmitic acid (PA, 16:0), i.e., stearoyl-ACP desaturase (SAD) and palmitoyl-ACP desaturase (PAD), respectively [3]. In contrast to the conservation of soluble FADs, membrane-bound FADs are highly diverse, including FAD2, FAD6, FAD3, FAD7/8, FAD4, acyl-coenzyme A (CoA) desaturase-like (ADS)/FAD5, sphingolipid delta8-desaturase (SLD), and sphingolipid delta4-desaturase (DES), which exist in the endoplasmic reticulum (ER) or plastid membranes [2]. Microsomal FAD2s and plastidial FAD6s are Δ12 FADs that convert oleic acid (OA, 18:1) into linoleic acid (LA, 18:2), whereas FAD3 (microsomal) and FAD7/8 (plastidial) are Δ15 FADs that catalyze LA into α-linolenic acid (LA, 18:3) in the ER and chloroplasts, respectively. Whereas FAD5 and its homologs in Arabidopsis (*Arabidopsis thaliana*) convert C16:0 into palmitoleic acid (C16:1) in both the ER and chloroplast [4, 5], FAD4 introduces a Δ3 *trans* double bond at palmitate at the sn-2 position of phosphatidylglycerol in the chloroplast [6]. SLD and DES introduce double bonds in sphingolipids, resulting in 8 (Z/E)-C18-phytosphingenine and sphinga-4,8-dienine, respectively [7, 8]. Besides Arabidopsis, membrane-bound FADs have also been characterized in several other plant species, e.g., rapeseed (*Brassica napus*), grapevine (*Vitis vinifera*), cotton (*Gossypium hirsutum*), poplar (*Populus trichocarpa*), sunflower (*Helianthus annuus*), oil tea (*Camellia oleifera*), olive (*Olea europaea*), rice (*Oryza sativa*), and barley (*Hordeum vulgare*) [9–17]. Nevertheless, no information is available in Cyperaceae plants, which comprise the second largest family within the Poales order [18].

Tigernut (*Cyperus esculentus* L. var. *sativus* Baeck.) is a novel oilcrop that belongs to the Cyperaceae family [19–21]. Unlike traditional oilcrops producing oil in seeds or fruits, tigernut accumulates up to 35% of oil in its underground tubers [22–24]. Interestingly, the composition of tigernut oil is highly similar to oil tea and olive, possessing 62.3–74.6% 18:1, 12.2–16.2% 16:0, 8.8–18.0% 18:2, 1.1–4.9% 18:0, and 0.2–2.4% 18:3 [25–28]. However, thus far, genes contributing to oil accumulation and FA composition have not been well studied in this species, though six genes encoding soluble FADs have been described [29, 30]. In this study, we took advantage of the recently available genome [31] to identify the complete set of genes encoding membrane-bound FADs in tigernut. In contrast to the absence of an FAD5 homolog, phylogenetic and orthologous analyses revealed species or lineage-specific expansion of FAD2 and SLD in tigernut, which were contributed by tandem and dispersed duplications, respectively. Moreover, our comparative genomics analysis indicated that FAD3 and −7 are more likely to arise from segmental duplication, where *CeFAD7* appears to play a more important role in tigernut. Expression analyses also uncovered species-specific enhancement of certain *CeFAD* genes, which may explain the distinct FA composition between tigernut and its close relative purple nutsedge (*C. rotundus*). Herein, we report our findings.

Results

Identification, phylogeny, chromosomal localization, and duplication event analysis of ten *FAD* genes in tigernut

Homologue search of the tigernut genome using AtFADs resulted in ten genes that encode membrane-bound FADs, which were named following their counterparts in Arabidopsis, i.e., *CeFAD2-1–3*, *CeFAD6*, *CeFAD3*, *CeFAD7*, *CeFAD4*, *CeDES1*, and *CeSLD1–2*. An unrooted evolutionary tree with 18 AtFADs is shown in Fig. 1a. Notably, despite the presence of nine ADSs in Arabidopsis (since their homologs identified in other species are most close to AtFAD5, this group was named FAD5 for convenience), no counterpart was detected in tigernut. By contrast, 1:1, 1:3, 2:1, and 2:2 orthologous

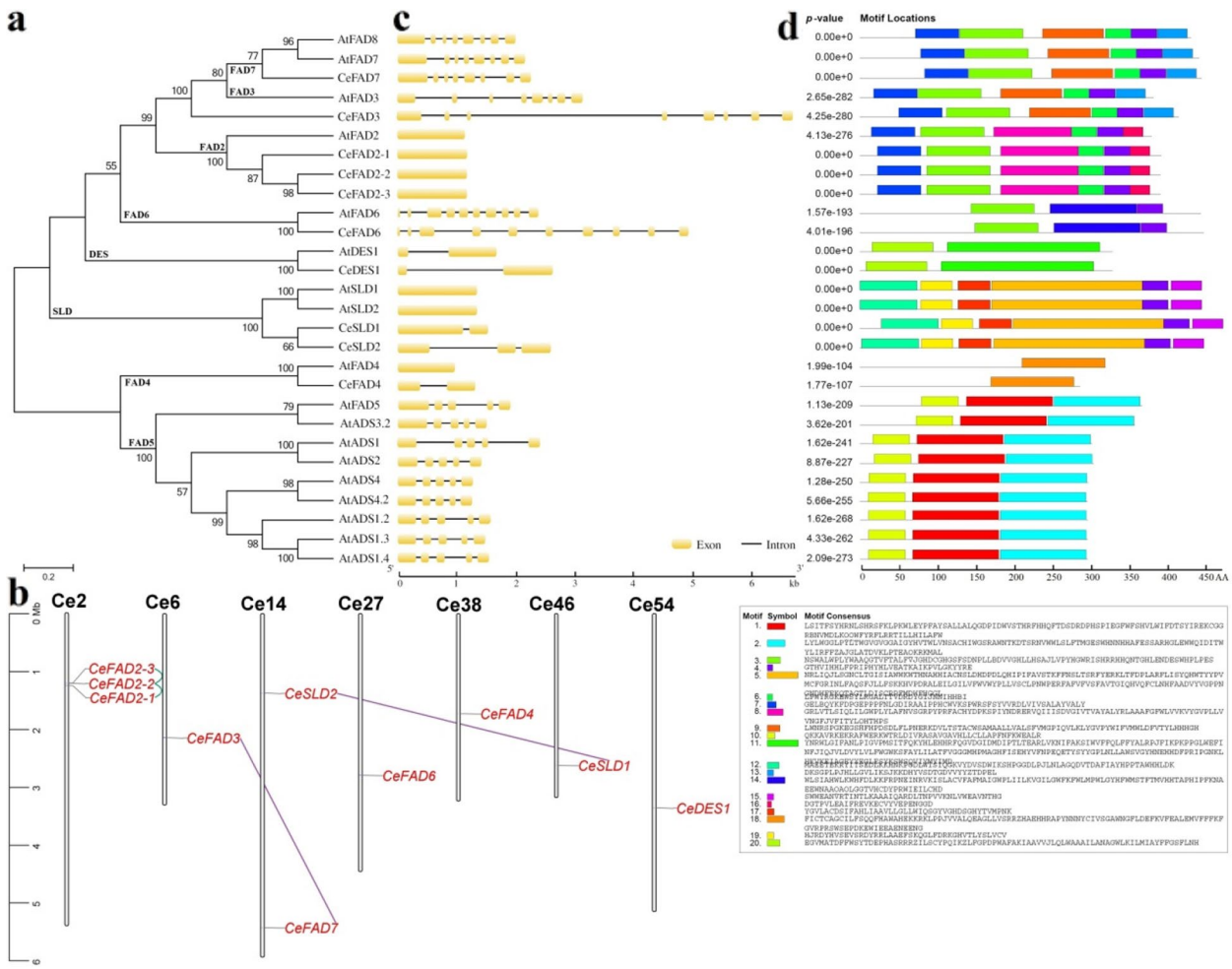

Fig. 1 Phylogenetic, structural, and duplication event analyses of genes encoding membrane-bound FADs in tigernut. **a** Shown is an unrooted phylogenetic tree resulting from full-length Ce/AtFAD proteins with MEGA6 (maximum likelihood method and bootstrap of 1,000 replicates), where the distance scale denotes the number of amino acid substitutions per site. The name of each clade is indicated next to the corresponding group. **b** Shown are chromosomal localization and duplication events of *CeFAD* genes, where dispersed and tandem repeats are connected using purple and blue lines, respectively. The serial number of each scaffold is indicated at the top, whereas the scale is in Mb. **c** Shown are the exon–intron structures. **d** Shown is the distribution of conserved motifs among Ce/AtFAD proteins, where different motifs are represented by different color blocks as indicated and the same color block in different proteins indicates a certain motif. (*ADS* acyl-coenzyme A desaturase-like, *At A. thaliana*, *Ce C. esculentus*, *DES* sphingolipid delta4-desaturase, *FAD* fatty acid desaturase, *Mb* megabase, *SLD* sphingolipid delta8-desaturase)

relationships were observed for other members between Arabidopsis and tigernut, implying species or lineage-specific expansion and contraction (Fig. 1a).

Further chromosomal localization showed that ten *CeFAD* genes are distributed over seven scaffolds (Scfs), i.e., Scf2, Scf6, Scf14, Scf27, Scf38, Scf46, and Scf54 (Fig. 1b). Whereas most scaffolds contain a single member, Scf14 and Scf2 harbor two (i.e., *CeFAD7* and *CeSLD2*) and three (i.e., *CeFAD2-1*, *−2*, and *−3*), respectively. Among them, *CeFAD2-1*, *−2*, and *−3* are organized in tandem repeats, exhibiting 87.63–94.94% sequence similarities at the protein level, relatively higher than 75.95–80.05% with AtFAD2 (Additional file 1), implying species or lineage-specific expansion. Notably, in contrast to *AtFAD7/−8*, *AtADS1/−2*, and *AtSLD1/−2* that were characterized as whole-genome duplication (WGD, α) repeats (Additional file 2), no *CeFAD* genes were shown to locate within syntenic blocks (see below). Instead, *CeFAD3/−7* and *CeSLD1/−2*, which share 69.59% and 73.28% sequence similarities at the protein level, respectively, were characterized as dispersed repeats (Fig. 1b). Among them, CeFAD7 was shown to exhibit 77.46% and 77.06% sequence similarities with AtFAD7 and AtFAD8, respectively, which are relatively higher than 66.96% with AtFAD3. Interestingly, *CeFAD7* and *AtFAD3* was shown to locate within syntenic blocks (see below), implying

Table 1 Genes encoding membrane-bound FADs identified in tigernut. (*AA* amino acid, *Ce C. esculentus*, *Cyt-b5* cytochrome b5-like heme/steroid binding, *DES* sphingolipid delta4-desaturase, *DUF3474* domain of unknown function, *FAD* fatty acid desaturase, *GRAVY* grand average of hydropathicity, *kDa* kilodalton, *Lipid_DES* sphingolipid delta4-desaturase, *TMEM189_B* B domain of the transmembrane protein TMEM189, *MW* molecular weight, *pI* isoelectric point, *Scf* scaffold, *SLD* sphingolipid delta8-desaturase, *TMH* transmembrane helix)

Gene name	Locus ID	Position	AA	MW (kDa)	pI	GRAVY	TMH	DUF3474	FA_desaturase	TMEM189_B	Lipid_DES	Cyt-b5
CeFAD2-1	CESC_14206	Scf2:1,257,868..1261891(+)	396	45.31	8.96	−0.022	6	27..71	93..354	-	-	-
CeFAD2-2	CESC_14204	Scf2:1,219,192..1220379(+)	395	45.04	8.65	−0.035	5	26..70	93..354	-	-	-
CeFAD2-3	CESC_14203	Scf2:1,212,654..1213826(+)	395	45.47	8.48	−0.042	5	28..70	93..354	-	-	-
CeFAD6	CESC_10102	Scf27:2,791,409..2796371(+)	452	52.27	9.07	−0.209	2	-	153..401	-	-	-
CeFAD3	CESC_12151	Scf6:2,140,894..2147643(-)	419	48.17	8.92	−0.237	3	20..104	119..370	-	-	-
CeFAD7	CESC_13330	Scf14:5,424,469..5426736(-)	449	50.90	8.51	−0.176	3	1..138	145..401	-	-	-
CeFAD4	CESC_20996	Scf38:1,729,293 1,730,613(+)	289	31.84	8.64	0.058	3	-	-	95..264	-	-
CeDES1	CESC_21909	Scf54:3,356,295 3,359,126(+)	332	38.48	8.75	−0.024	4	-	71..296	-	13..48	-
CeSLD1	CESC_04819	Scf46:2,623,158 2,624,696(+)	477	53.93	9.35	0.048	4	-	168..435	-	-	40..109
CeSLD2	CESC_13801	Scf14:1,374,633 1,377,240(-)	452	51.74	8.96	−0.018	5	-	143..412	-	-	13..83

that *CeFAD7* and *CeFAD3* may arise from WGD or segmental duplication followed by species or lineage-specific chromosome rearrangement.

The physiochemical parameters of deduced CeFAD proteins are summarized in Table 1, where the peptide length varies from 289 (CeFAD4) to 477 (CeSLD1) amino acids (AA) with the molecular weight (MW) of 31.84–53.93 kilodalton (kDa). The values of theoretical isoelectric point (pI) are all greater than 7.0 (8.44–9.35), and the grand average of hydropathicity (GRAVY) values are less than 0 (from −0.022 to −0.237) with the exception of CeFAD4 and CeSLD1 (Table 1), implying the basic and hydrophilic features. The predicted transmembrane helices (TMH) vary from two to six. Except for CeFAD4, all other members include one FA_desaturase (fatty acid desaturase, under the Pfam accession number of PF00487) domain. Moreover, CeFAD2-1–3, CeFAD3, and CeFAD7 contain one DUF3474 domain (domain of unknown function, PF11960); CeDES1 has one Lipid_DES domain (sphingolipid delta4-desaturase, PF08557); and CeSLD1 and −2 possess one Cyt-b5 domain (cytochrome b5-like heme/steroid binding domain, PF00173) that includes the highly conserved HPGG motif at the N-terminus. Instead, CeFAD4 harbors one TMEM189_B dmain (B domain of the transmembrane protein TMEM189, PF10520) or Lipid_desat domain (lipid desaturase) (Table 1 and Additional file 3). Though the overall sequence similarities are relatively low (see Additional file 1), all of them harbor three conserved histidine-boxes that could potentially coordinate a metal centre involved in catalysis, i.e., HxxxH, HxxxH, and HxxHH, in contrast to an xxHH variant observed at the first histidine-box of CeFAD4 (Additional file 3). Additionally, an ER retention signal F/YNNKF was observed at the N-terminus of three CeFAD2s (Additional file 3).

Analyzing gene structure revealed that the intron amounts of *CeFAD* genes vary from zero to nine. The exon–intron structures are highly conserved in several evolutionary groups, i.e., FAD2, DES, FAD5, FAD3/7, and FAD6, which feature zero, one, four, seven, and nine introns, respectively. By contrast, compared with Arabidopsis, more introns were found for other groups in tigernut, i.e., FAD4 (0 vs 1) and SLD (0 vs 1/2) (Fig. 1c). Interestingly, the exon–intron structures were shown to be highly conserved in all Cyperaceae and Juncaceae plants examined in this study (Additional file 4), implying lineage-specific gain. Moreover, conserved motifs are conserved within a group but usually differ between evolutionary groups. Among 20 motifs identified in this study, Motifs 3, 4, 6, and 7 are widely distributed, whereas others are group-specific. All members in FAD3 and FAD7 possess Motifs 7, 3, 9, 6, 4, and 13, where Motifs 9 and 13 are placed by Motifs 8 and 16 in FAD2, respectively. By contrast, FAD6 features Motifs 3, 14, and 4, where Motif 14 is group-specific. Besides Motif 4, all SLDs possess five group-specific motifs, i.e., 12, 19, 17, 5, and 15. FAD5 features Motifs 10, 1, and 2, DES features Motifs 20 and 11, and FAD4 possesses Motif18, all of which are group-specific (Fig. 1d). Among them, Motifs 3, 8, 9, 6, 11, 14, 4, 5, and 17 belong to the FA_desaturase domain, whereas Motifs 7, 12, and 20 were characterized as the DUF3474, Cyt-b5 and Lipid_DES domain, respectively. Additionally, the chloroplast transit peptide present in the N-terminal of FAD4s, FAD6s, and FAD7s was not identified by our MEME analysis, mainly due to sequence diversification and only 20 motifs identified in this study.

Characterization of *FAD* genes from representative plant species and insights into lineage-specific family evolution in Cyperaceae

Above phylogenetic analysis suggests that early divergence of *FAD* genes into eight groups (i.e., FAD2, FAD6, FAD3, FAD7, FAD4, FAD5, DES, and SLD) may occur sometime before monocot-eudicot split. However, there are four issues that still need to be resolved: 1) the loss of FAD5 in tigernut is species or lineage-specific; 2) expansion of FAD2 in tigernut is species or lineage-specific; 3) the exact origin of FAD3 and −7; 4) the exact origin of *CeSLD1* and −*2*. For the purposes, homologs were further identified from representative plant species, which include *Chlamydomonas reinhardtii* (a single celled green alga in Chlamydomonadales), moss (*Physcomitrium patens*, an early coloned nonvascular land plant in Funariales), spikemoss (*Selaginella moellendorffii*, an ancient vascular plant in Selaginellales), Western redcedar (*Thuja plicata*, a gymnosperm plant in Cupressales), *Amborella trichopoda* (the basal angiosperm in Amborellales), and three early diverged monocots that didn't experience the so-called τ WGD, i.e., *Acorus gramineus* (an Acoraceae plant in Acorales), eelgrass (*Zostera marina*, a Zosteraceae plant in Alismatales), and duckweed (*Spirodela polyrhiza*, an Araceae plant in Alismatales) [32–35]. As shown in Additional file 4, seven members identified in *C. reinhardtii* belong to FAD2, FAD6, FAD7, FAD4, FAD5, and SLD, supporting early divergence of these six groups. DES seems to first appear in moss, and a FAD3 homolog was first detected in gymnosperm (*T. plicata*), where TpFAD3 shares 63.45% sequence similarity with TpFAD7, relatively smaller than 70.39% observed between AtrFAD3 and AtrFAD7. Notably, despite early origin of FAD5, it was shown to be absent from *T. plicata*, *A. trichopoda*, and all core monocots examined in this study. Since *A. gramineus*, eelgrass, and duckweed all contain one FAD5, its loss in core monocots is more likely to be lineage-specific, occurred sometime before

monocot radiation. On the contrary, SLD seems to have expanded along with the monocot radiation, usually present in two subgroups (i.e., SLD1 and −2) as observed in tigernut, though SLD2 is absent from three Juncaceae species examined in this study, i.e., *Juncus effusus*, *J. inflexus*, and *Luzula sylvatica* (Additional file 4).

To learn more about lineage-specific evolution of *FAD* genes, orthologous genes among different species were identified using Orthofinder, which resulted in 11 orthogroups (Fig. 2). Whereas a single member was found for FAD3, FAD6, FAD7, FAD4, FAD5, and DES in tigernut, two and three were identified for SLD and FAD2, respectively. Notably, all three *CeFAD2* genes belong to FAD2a, implying species-specific expansion. Correspondingly, only one FAD2 was identified from the tuber transcriptome assembly of purple nutsedge (Additional file 4), a species standing very close to tigernut [36–38]. By contrast, *FAD2* genes in *C. breviculmis*, *C. littledalei*, and *C. scoparia* belong to FAD2a, FAD2b, and FAD2c, where FAD2b was also shown to be present in *R. breviuscula* and *R. tenuis*, implying its early divergence before the *Rhynchospora-Carex* split. Notably, despite the presence of four *FAD2* genes in both *C. littledalei* and *C. scoparia*, 1:1 and 2:2 orthologous relationships were observed, implying their different origins. In *C. littledalei*, *ClFAD2-1*, *−2*, and *−3* are organized as tandem repeats, whereas *ClFAD2-4* was characterized as a dispersed repeat of *ClFAD2-1*. By contrast, *CsFAD2-2* and *−4* in *C. scoparia* were characterized as dispersed repeat of *CsFAD2-1*, while *CsFAD2-2* and *−3* are organized as tandem repeats, implying species-specific expansion. Interestingly, like high sequence identity of 99.10% observed between *ClFAD2-1* and *−2*, *CsFAD2-2* exhibited 97.00% identity with *ClFAD2-1*, considerably higher than 71.70% with *CsFAD2-3*, supporting recent origin of *ClFAD2-1* and *CsFAD2-1*. Among two SLDs identified in this study, SLD1 was shown to be widely distributed, whereas SLD2 is limited to core monocots but not three early diverged monocots, i.e., *A. gramineus*, eelgrass, and duckweed, implying its birth along with the τ WGD shared by core monocots [39]. This means that the last common ancestor of core monocots contains eight orthogroups, i.e., FAD2, FAD6, FAD3, FAD7, FAD4, DES, SLD1, and SLD2. Since SLD1 members in other species feature no intron, gain of the intron in Juncaceae and Cyperaceae plants may occur sometime after their split with other families in Poales. By contrast, two models could be speculated for SLD2, which feature two introns in all tested Cyperaceae plants: 1) gain of these two introns occurred in the last common ancestor of Juncaceae and Cyperaceae, followed by Juncaceae-specific loss of SLD2; 2) the event is Cyperaceae-specific, occurred sometime after the split with Juncaceae, whereas Juncaceae experienced lineage-specific loss of SLD2.

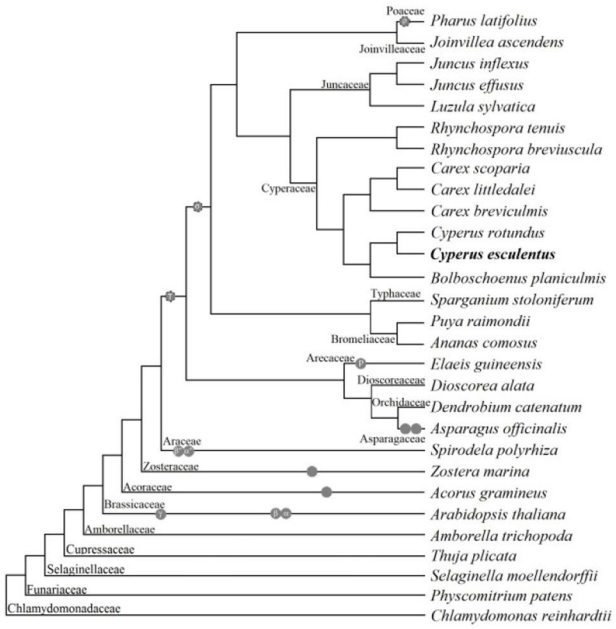

FAD2a	FAD2b	FAD2c	FAD6	FAD7	FAD3	FAD4	FAD5	DES	SLD1	SLD2	Total
1	0	0	1	2	2	1	0	2	1	1	11
1	0	0	1	1	1	1	0	1	1	1	8
1	0	0	1	1	1	2	0	1	1	0	8
1	0	0	1	1	1	1	0	1	1	0	7
5	0	0	1	1	1	1	0	1	1	0	11
3	0	0	1	1	1	1	0	1	1	1	10
2	0	0	1	1	1	1	0	1	1	1	9
2	1	1	1	1	1	1	0	1	1	1	11
2	1	1	1	1	1	1	0	1	1	1	11
1	1	1	1	1	1	1	0	1	1	1	10
1	0	0	1	1	1	0	0	1	1	1	7
3	0	0	1	1	1	1	0	1	1	1	10
1	0	0	1	1	1	1	0	1	1	1	8
2	0	0	1	2	1	1	0	2	1	1	11
1	0	0	1	1	1	1	0	1	1	1	8
1	0	0	1	1	1	1	0	1	1	1	8
2	0	0	1	2	1	1	0	2	1	2	12
3	0	0	1	1	2	1	0	1	0	2	11
2	0	0	2	4	0	0	0	1	2	0	11
2	0	0	1	1	1	1	0	1	1	1	9
1	0	0	1	1	1	1	1	1	1	0	8
1	0	0	1	1	2	1	1	1	1	0	9
2	0	0	1	3	0	1	1	1	2	0	11
1	0	0	1	2	1	1	9	1	2	0	18
1	0	0	1	1	1	1	0	1	1	0	7
2	0	0	1	1	1	1	0	0	1	0	7
1	0	0	4	1	0	1	1	1	2	0	11
2	0	0	3	6	0	1	2	1	1	0	16
1	0	0	1	1	0	1	2	0	1	0	7

Fig. 2 Species-specific distribution of 11 orthogroups in 29 representative plant species. The species tree is referred to NCBI Taxonomy (https://www.ncbi.nlm.nih.gov/taxonomy) and well-established recent whole-genome duplications are marked. Names of tested plant families are indicated next to the corresponding branches. (*ADS* acyl-coenzyme A desaturase-like, *DES* sphingolipid delta4-desaturase, *FAD* fatty acid desaturase, *SLD* sphingolipid delta8-desaturase)

To gain insights into the origin of *FAD* genes, species-specific duplication events and interspecific syntenic analyses were further investigated. Whereas no syntenic relationship was detected between *FAD* genes in all Cyperaceae and Juncaceae plants, one to six pairs of WGD repeats were identified in Arabidopsis, *A. gramineus*, *Dioscorea alata*, oil palm (*Elaeis guineensis*), pineapple (*Ananas comosus*), *Sparganium stoloniferum*, *Joinvillea ascendens*, and *Pharus latifolius* (Additional file 4). Late origin of FAD3 in gymnosperm and location of *EgFAD3/7-1/7-2*, *AcFAD3/−7*, *JaFAD3/−7*, and *PlFAD7-1/3-1/3-2* implied segmental duplication-derivation of FAD3 from FAD7. Correspondingly, interspecific syntenic analyses revealed that *CeFAD7* exhibited 1:2, 1:3, or 1:4 syntenic relationships with FAD7 and FAD3 members in a high number of species examined in this study, e.g., *C. littledalei*, *Rhynchospora breviuscula* (Fig. 3a), *J. effusus*, pineapple, *S. stoloniferum* (Fig. 3b), *J. ascendens*, *P. latifolius*, and oil palm (Fig. 3c). Moreover, *EgSLD1*, *-2a*, and *-2b* were also shown to locate within syntenic blocks (Fig. 3c), providing direct evidence of SLD2 from SLD1 via the τ WGD followed by lineage-specific expansion of *EgSLD2b* from *-2a* via the Arecaceae-specific p WGD. Interestingly, except for *CeFAD2-1* and *CeFAD2-2*, all other *CeFAD* genes were shown to have syntelogs in at least one out of 27 species examined in this study. In contrast to only *CeFAD7* and *CeFAD4* that have syntelogs in Arabidopsis, i.e., *AtFAD3* and *AtFAD4*, respectively (Fig. 3d), nearly 1:1 syntenic relationships were observed between tigernut and other Cyperaceae species, i.e., *C. littledalei*, *C. scoparia*, and *R. breviuscula* (Fig. 3a), reflecting their close biological relationships and implying functional conservation of related genes. Compared with Arabidopsis, besides *CeFAD7/-4*, *CeFAD2-3* and *CeDES1* were also shown to have syntelogs in both *A. gramineus* and *A. trichopoda*, though FAD2 has expanded via WGD in *A. gramineus* (Fig. 3d).

Tissue-specific transcriptome profiling revealed distinct expression patterns of *CeFAD* genes

To provide a global view of expression profiles of *CeFAD* genes, seven main tissues or developmental stages, i.e., shoot apex, young leaf, mature leaf, sheath, root, rhizome, and tuber, were first investigated using RNA-seq data. As shown in Fig. 4a, despite the expression of all ten *CeFAD* genes identified in this study, distinct expression patterns were observed. Whereas *CeFAD2-1*, *CeFAD6*, and *CeFAD7* were shown to be constitutively expressed, others seem to be tissue-specific. *CeFAD2-1* was expressed mostly in tubers, reflecting high oil accumulation in this tissue [40]. By contrast, its two paralogs *CeFAD2-2* and *CeFAD2-3* were lowly expressed in most tissues examined in this study, though the latter exhibited a tissue-specific expression pattern in shoot apex and rhizome. The transcripts of *CeFAD6* were most abundant in leaves and sheaths, followed by roots, rhizomes, and shoot apexes, and least in tubers, whereas *CeFAD7* transcripts were mostly found in shoot apexes, followed by rhizomes, tubers, roots, and leaves, and least in sheaths. *CeDES1* was expressed in most tested tissues, but barely in mature leaf. Whereas *CeFAD3* was preferentially expressed in roots, rhizomes, and shoot apexes, *CeFAD4* was predominantly expressed in young leaves, mature leaves, and sheaths. *CeSLD1* was expressed mostly in tubers, followed by young leaf, sheath, roots, and shoot apexes, but rarely in rhizomes and mature leaves. Compared with *CeSLD1*, the transcript levels of *CeSLD2* were relatively less in most tissues with the exception of mature leaf, implying their divergence.

According to the transcript abundance, several key members were identified in a certain tissue. Among them, *CeFAD7* represented the most expressed member in all tested tissues with the exception of the oil-bearing tuber, where *CeFAD2-1* was most abundant. Whereas *CeFAD7* occupied 86.11% of total *CeFAD* transcripts in shoot apexes, *CeFAD7* and *CeFAD2-1* contributed to 92.22%, 91.37%, and 80.15% of those in rhizomes, tubers, and roots, respectively. In young leaves, 88.66% of total *CeFAD* transcripts were contributed by *CeFAD7*, *CeFAD2-1*, and *CeFAD6*, whereas 92.45% of those in mature leaves were contributed by *CeFAD7*, *−4*, and *−6*. In sheaths, 90.19% of total *CeFAD* transcripts were contributed by *CeFAD7*, *CeFAD2-1*, *CeFAD6*, and *CeSLD1* (Fig. 4a).

According to the expression patterns, ten *CeFAD* genes were clustered into three main groups. Group I includes *CeFAD7* and *CeFAD2-1* that were constitutively and highly expressed in all tested tissues. Group II contains two subgroups: whereas Group IIa includes *CeFAD3* that exhibited a tissue-specific expression pattern in roots, rhizomes, and shoot apexes, Group IIb contains *CeFAD2-2* and *CeFAD2-3* that were lowly expressed in most tissues. Group III includes three subgroups: Group IIIa includes *CeFAD4* that exhibited a tissue-specific expression pattern in in leaves and sheaths; Group IIIb includes *CeFAD6* that was constitutively expressed; Group IIIc includes *CeSLD1*, *CeDES1*, and *CeSLD2* (Fig. 4a).

Comparative analysis revealed expression divergence of *FAD* genes between tigernut and purple nutsedge

Unlike tigernut, purple nutsedge tubers are poor in oil accumulation, which also exhibits distinct FA composition [25, 28]. To uncover the underlying mechanism, expression profiles of *Ce*/*ClFAD* genes were compared across three swelling stages of tuber development, i.e., 20, 50, and 90 days after tuber initiation (DAI). Since no

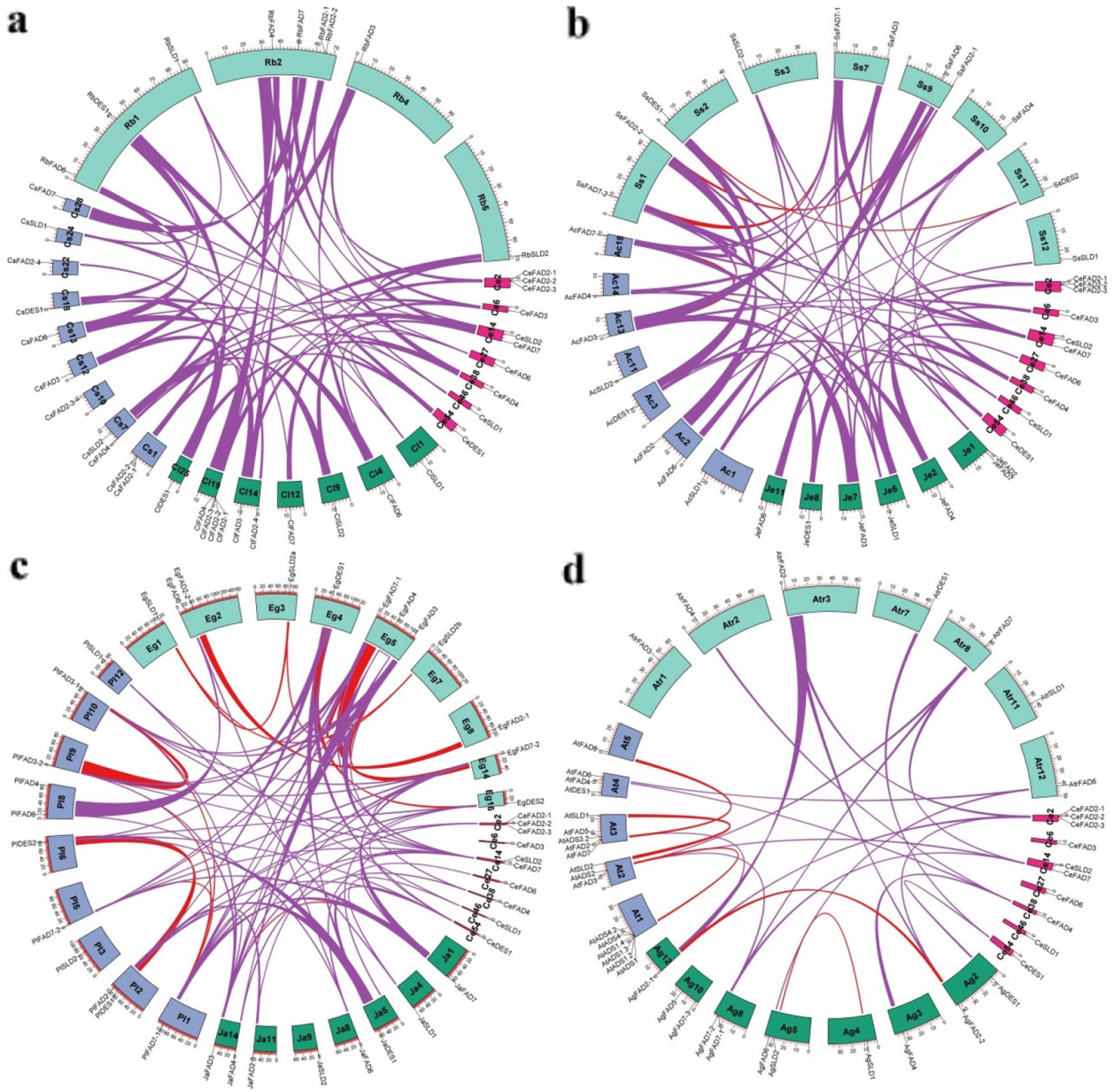

Fig. 3 Synteny analyses within and between tigernut and representative plant species. **a** Synteny analysis within and between tigernut, *C. littledalei*, *C. scoparia*, and *R. breviuscula*. **b** Synteny analysis within and between tigernut, *J. effusus*, *A. comosus*, and *S. stoloniferum*. **c** Synteny analysis within and between tigernut, *J. ascendens*, *P. latifolius*, and *E. guineensis*. **d** Synteny analysis within and between tigernut, *A. gramineus*, *A. thaliana*, and *A. trichopoda*. Shown are *FAD* gene-encoding chromosomes/scaffolds and only syntenic blocks containing *FAD* genes are marked, where red and purple lines indicate intra- and inter-species, respectively. The scale is in Mb. (*Ac A. comosus*, *ADS* acyl-coenzyme A desaturase-like, *Ag A. gramineus*, *At A. thaliana*, *Atr A. trichopoda*, *Ce C. esculentus*, *Cl C. littledalei*, *Cs C. scoparia*, *DES* sphingolipid delta4-desaturase, *Eg E. guineensis*, *FAD* fatty acid desaturase, *Ja J. ascendens*, *Je J. effuses*, *Mb* megabase, *Pl P. latifolius*, *Rb R. breviuscula*, *SLD* sphingolipid delta8-desaturase, *Ss S. stoloniferum*)

counterparts for *CeFAD2-2*, *CeFAD2-3*, and *CeFAD4* were identified from the purple nutsedge transcriptome, their coding sequences were employed for read mapping. As expected, no mapping reads were detected for these three genes, implying that they may not exist in the purple nutsedge genome or only express in specific tissues beyond the tuber or certain stages of organ development. Moreover, apparent expression divergence was observed between tigernut and purple nutsedge orthologs. As shown in Fig. 4b, compared with their orthologs in tigernut, *CrFAD2*, *CrFAD6*, and *CrSLD1* were expressed considerably less at nearly all three tested stages, whereas

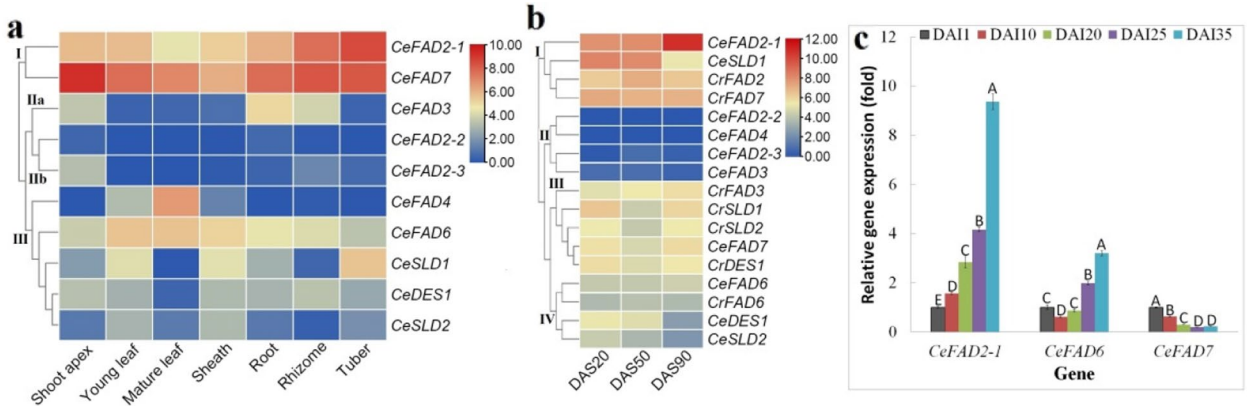

Fig. 4 Expression profiles of *FAD* genes in tigernut and purple nutsedge. **a** Tissue-specific expression profiles of ten *CeFAD* genes. **b** Expression profiles of *Ce/CrFAD* genes at three representative stages of tuber development. **c** Expression profiles of *CeFAD2-1*, *CeFAD6*, and *CeFAD7* at different stages of tuber development. The heatmap was generated using the R package implemented with a row-based standardization. Color scale represents FPKM normalized $\log_2$ transformed counts, where blue indicates low expression and red indicates high expression. Bars indicate SD (N = 3) and uppercase letters indicate difference significance tested following Duncan's one-way multiple-range post hoc ANOVA ($P < 0.01$). (*ADS* acyl-coenzyme A desaturase-like, *Ce C. esculentus*, *Cr C. rotundus*, *DAI* days after tuber initiation, *DES* sphingolipid delta4-desaturase, *FAD* fatty acid desaturase, *FPKM* Fragments per kilobase of exon per million fragments mapped, *SLD* sphingolipid delta8-desaturase)

CrFAD3, *CrFAD7*, *CrDES1*, and *CrSLD2* exhibited an opposite trend. Interestingly, according to the cluster analysis, *CeFAD2-1*, *CeSLD1*, *CrFAD7*, and *CrFAD2* appeared in Group I that were highly abundant in tubers, in striking contrast to rare expression of *CeFAD2-2*, *CeFAD2-3*, *CeFAD3*, and *CeFAD4* in Group II. Group III includes *CeFAD7*, *CrFAD3*, *CrSLD1*, *CrSLD2*, and *CrDES1*, whereas Group IV includes *CeFAD6*, *CrFAD6*, *CeDES1*, and *CeSLD2* that exhibited moderate expression (Fig. 4b).

Expression profiles of *CeFAD2-1*, *CeFAD6*, and *CeFAD7* during tuber development

To learn more about expression profiles of *CeFAD* genes during tuber development, three key members (i.e. *CeFAD2-1*, *CeFAD6*, and *CeFAD7*) that may contribute oil accumulation and FA composition were further checked using qRT-PCR. Five stages examined in this study are as previously described, which represent tuber initiation (1 DAI), early swelling (10 DAI), middle swelling (20 DAI), late swelling (25 DAI), and maturation (35 DAI), respectively [40, 41]. It's worth noting that the whole growth period of Reyan3 observed in this study (Hainan) was about 85 d, relatively shorter than approximately 150 d as described in other regions such as Beijing and Jilin [25, 26, 40]. As shown in Fig. 4c, *CeFAD2-1* transcripts gradually increased along with tuber development, peaking at 35 DAI, whereas *CeFAD6* transcripts initially decreased at 10 DAI followed by gradual enhancement during latter development, also peaking at 35 DAI (Fig. 4b). Their expression patterns are largely in accordance with transcriptome profiling (Fig. 4b). By contrast, *CeFAD7* transcripts were shown to peak at 1 DAI, followed by gradual decrease during latter development (Fig. 4c), which is something different from a U trend as observed by transcriptome profiling (Fig. 4b), possiblely due to different varieties and growing conditions adopted [25, 39]. These results imply a more important role of *CeFAD2-1* than *CeFAD6* and *CeFAD7* in oil accumulation of tigernut tubers.

Discussion

The importance of membrane-bound FADs especially FAD2/−3 in determining FA composition [42–44] impelled us to conduct a comprehensive analysis of this special family in tigernut, a unique oil-rich tuber plant in the Cyperaceae family [22, 40]. Mining the tigernut genome resulted in ten members, and the family amounts are comparable to 10–12 reported in barley, rice, and grapevine, but considerably less than 18–68 described in Arabidopsis, poplar, oil tea, olive, cotton, sunflower, and rapeseed [9–17]. Phylogenetic analysis assigned ten *CeFAD* genes into seven out of eight evolutionary groups as defined in Arabidopsis, i.e., FAD2 (3), FAD6 (1), FAD3 (1), FAD7 (1), FAD4 (1), DES (1), and SLD (2). In accordance with those reported in barley and rice [10, 16], no FAD5 was identified in tigernut. By contrast, both FAD2 and SLD have expanded in this species, which were shown to be contributed by tandem and dispersed duplications, respectively.

To learn more about the origin and evolution of *CeFAD* genes, a total of 285 homologs were further identified from 29 representative plant species, which belong to 18 plant families, i.e., Chlamydomonadaceae (1), Funariaceae

(1), Selaginellaceae (1), Cupressaceae (1), Amborellaceae (1), Acoraceae (1), Zosteraceae (1), Araceae (1), Asparagaceae (1), Orchidaceae (1), Dioscoreaceae (1), Arecaceae (1), Bromeliaceae (2), Typhaceae (1), Cyperaceae (9), Juncaceae (3), Joinvilleaceae (1), and Poaceae (1). In contrast to the absence of any recent WGD in the basal angiosperm *A. trichopoda* [35], the model eudicot Arabidopsis was proven to have experienced three WGDs after monocot-eudicot divergence, which are known as γ, β, and α in sequence [45]. Similarly, Poaceae plants represented by *P. latifolius* also underwent three WGDs (i.e., τ, σ, and ρ) after the split with the eudicot clade [39]. Whereas σ and ρ WGDs are specific to Poales and Poaceae, respectively, the τ WGD is shared by all core monocots but not three early diverged monocots examined in this study, i.e., *A. gramineus* in Acoraceae, *Z. marina* in Zosteraceae, and *S. polyrhiza* in Araceae, which experienced one or two lineage-specific WGDs [32–34]. According to orthologous analysis, *FAD* genes identified in this study were clustered into 11 orthogroups, i.e., FAD2a, FAD2b, FAD2c, FAD6, FAD7, FAD3, FAD4, FAD5, DES, SLD1, and SLD2. Presence of FAD2a, FAD6, FAD7, FAD4, FAD5, and SLD1 in *C. reinhardtii* supports their early origin, whereas DES and FAD3 seem to be relatively younger, first appearing in moss and *T. plicata*, respectively. Our results indicated that all eight evolutionary groups found in Arabidopsis have already appeared in the last common ancestor of seed plants, which were followed by lineage-specific expansion and contraction during latter evolution. A good example for lineage-specific gene contraction is the loss of FAD5 in *A. trichopoda* and all core monocots examined in this study, which include tigernut. By contrast, this group has extensively expanded via WGD, tandem, and dispersed duplications in Arabidopsis, resulting in a high number of nine members [5].

As for two evolutionary groups (i.e., FAD2 and SLD) that underwent expansion in tigernut, the mechanism of FAD2 is more likely to be species-specific, evidences are as follows: 1) only one member was identified in its two close relatives, i.e., purple nutsedge and *Bolboschoenus planiculmis*; 2) no mapping reads were found for *CeFAD2-2* and *CeFAD2-3* in three stages of tuber development available in purple nutsedge; 3) the expansion in other Cyperaceae species was shown to be genus or species-specific. Moreover, in other families within Poales, a single member that belong to FAD2a was also observed in a high number of tested species, i.e., *J. effuses* (Juncaceae), *J. inflexus* (Juncaceae), *J. ascendens* (Joinvilleaceae), *P. latifolius* (Poaceae), *A. comosus* (Bromeliaceae), and *P. raimondii* (Bromeliaceae), implying the presence of one FAD2 in the last common ancestor of Poales plants. On the contrary, though *CeSLD2* was characterized as a dispersed repeat of *CeSLD1*, they belong to SLD1 and SLD2, respectively, which were shown to be widely present in core monocots examined in this study. Since SLD2 is limited to core monocots and two members (*EgSLD2a* and *−2b*) present in oil palm are still located within syntenic blocks with the SLD1 member *EgSLD1*, it means that SLD2 is more likely to arise from SLD1 via the τ WGD, followed by lineage or species-specific chromosome rearrangement in most species. Interestingly, in contrast to lineage-specific expansion of SLD2 via the p WGD shared by all Arecaceae plants [46], in species such as Arabidopsis, *A. gramineus*, and *D. alata*, SLD1 was shown to further undergo species-specific expansion via recent WGDs [34, 45, 47]. Notably, our data suggests that the Poales-specific σ WGD had no effect on the family expansion in species examined in this study, which usually contain a single member for eight orthogroups, i.e., FAD2a, FAD6, FAD7, FAD3, FAD4, DES, SLD1, and SLD2. Besides WGD and dispersed duplication, local duplication such as tandem and proximal duplications also played a role in the family expansion, especially for FAD2 in tigernut and a high number of Cyperaceae plants, e.g., *C. littledalei*, *C. scoparia*, *R. breviuscula*, and *R. tenuis*.

Exon–intron structures of *FAD* genes are usually conserved within the same evolutionary group. Generally, FAD2, FAD4, and SLD are typical for no intron, whereas DES, FAD5, FAD3/7, and FAD6 feature one, four, seven, and nine introns, respectively. Interestingly, *CeFAD4*, *CeSLD1*, and *CeSLD2* were shown to have gain one, one, and two introns, resepectively, which are highly conserved in all Cyperaceae and Juncaceae plants examined in this study, implying lineage-specific gain of these introns. Though their biological significances are yet to be studied, similar cases have also been reported for genes in *SAD*, *oleosin*, and *aquaporin* families [30, 40, 41].

Generally, expression patterns reflect the functions of a gene in certain tissues and/or developmental stages, whereas expression divergence represents a key mechanism for neofunctionalization of duplicated genes or orthologs between different species [48]. Nearly 1:1 orthologous relationships observed between tigernut and other Cyperaceae plants imply the conservative functions of related *FAD* genes. Transcription of all ten *CeFAD* genes in at least one out of seven tested tissues suggests their putative roles in tigernut, whereas constitutive expression of *CeFAD2-1*, *CeFAD6*, and *CeFAD7* implies their essential roles in various tissues. Interestingly, transcript levels of *CeFAD2-1* were shown to gradually increase during tuber development, positively associated with oil accumulation [40]. Correspondingly, its transcripts in tubers were significantly more than those of the ortholog in purple nutsedge, i.e., *CrFAD2*. Given purple nutsedge tubers only producing less than 3% of oil [25, 28], species-specific enhancement of *CeFAD2-1*

transcripts may contribute to high oil accumulation in tigernut tubers. Actually, AtFAD2 was proven to be the key enzyme for PUFA biosynthesis in non-photosynthetic tissues such as developing seeds [49]. Notably, due to the lack of a whole genome for purple nutsedge, only seven *CrFAD* genes were identified from the tuber transcriptome, i.e., *CrFAD2*, *CrFAD6*, *CrFAD3*, *CrFAD7*, *CrDES1*, *CrSLD1*, and *CrSLD2*. Since FAD4 is widely distributed [6] and *CeFAD4* was shown to be preferentially expressed in photosynthetic tissues, no FAD4 homolog identified in purple nutsedge may attribute to the tissue-specific expression. Compared with their counterparts in tigernut, *CrSLD1* was expressed lower in the developing tubers, whereas others were expressed relatively more, which may contribute to the distinct FA composition between these two close species, e.g., 16.2% vs 32.6% C16:0, 1.1% vs 3.5% C18:0, 62.3% vs 26.9% C18:1, 18.0% vs 28.5% C18:2, and 2.4% vs 8.5% C18:3 [25]. Considering indispensable roles of FAD3 and −7 in C18:3 production [42, 50, 51], considerably less expression of *CeFAD3* and *CeFAD7* may explain the low level of 18:3 in tigernut tubers [25, 28], where *CeFAD3* is more likely to be the main contributor. Expression divergence was also observed for paralogs. Among two SLDs present in both tigernut and purple nutsedge, SLD1 has evolved into the predominant member, which is similar to three *CeFAD2* genes present in tigernut, where *CeFAD2-1* has become the dominant one.

Conclusions

This study presents the first genome-wide analysis of *FAD* genes in tigernut, an oil-rich tuber plant in Cyperaceae. A total of ten members were identified from the tigernut genome, representing seven evolutionary groups or eight orthogroups. Comparison of 285 members from 29 representative plant species supported that the last common ancestor of seed plants may include all eight evolutionary groups as defined in Arabidopsis. In contrast to species-specific expansion of FAD2, FAD5 loss and SLD expansion observed in tigernut appear to be lineage-specific, occurred sometime before monocot radiation. Syntenic analysis revealed segmental duplication-derivation of FAD3 from −7. Structural variation such as gain of introns and expression divergence of *CeFAD* genes were also observed, where *CeFAD2-1* and *CeSLD1* have evolved to be two predominant members. Expression analysis implied positive roles of *CeFAD2-1* in tuber oil accumulation, whereas low expression of *CeFAD3* may contribute to the distinct 18:3 content between tigernut and purple nutsedge tubers. These findings not only highlight lineage-specific evolution of the *FAD* family, but also provide valuable information for further functional analysis and genetic improvement in tigernut.

Materials and methods

Identification of *FAD* genes from datasets

Genome and transcriptome data of representative plant species were accessed from public databases such as Phytozome v13 (https://phytozome.jgi.doe.gov/pz/portal.html), Genome Warehouse (https://ngdc.cncb.ac.cn/gwh/), and NCBI (https://www.ncbi.nlm.nih.gov/): *C. reinhardtii* (v6.1), *P. patens* (v6.1), *S. moellendorffii* (v1.0), *T. plicata* (v3.1), *A. trichopoda* (v2.1), *A. thaliana* (Araport11), *A. gramineus* (v1), *Z. marina* (v3.1), *S. polyrhiza* (v2), *D. alata* (v2.1), *Dendrobium catenatum* (v1), *A. officinalis* (v1.1), *E. guineensis* (v3), *A. comosus* (v3), *Puya raimondii* (v1), *S. stoloniferum* (v1), *J. ascendens* (v1.1), *P. latifolius* (v1.1), *J. effusus* (v1), *J. inflexus* (v1), *L. sylvatica* (v1), *R. breviuscula* (v1), *R. tenuis* (v1), *C. breviculmis* (v2), *C. littledalei* (v1), *C. scoparia* (v1), *B. planiculmis* (v1), and *C. esculentus* (v1). Since genome sequences are not available for purple nutsedge, the de novo assembled tuber transcriptome as described before [40] was employed instead. tBLASTn [52] searching for homologs was conducted using reported AtFADs as queries, where the E-value was set to 1e−5. All candidates were checked using Pfam Search (http://pfam.xfam.org/) for the presence of the conserved FA_desaturase or TMEM189_B domains in deduced proteins. Gene structures were displayed using GSDS 2.0 (https://gsds.gao-lab.org/), whereas TMH and physiochemical parameters of deduced proteins were predicted using TMHMM-2.0 (https://services.healthtech.dtu.dk/services/TMHMM-2.0/) and ProtParam (http://web.expasy.org/protparam/), respectively.

Phylogenetic and conserved motif analyses

Multiple sequence alignments of deduced proteins were performed using MUSCLE implemented in MEGA6 [53], and phylogenetic tree construction was conducted using MEGA6 with the maximum likelihood method and bootstrap of 1,000 replicates. Protein domains were determined using Pfam Search and conserved motifs were identified using MEME (v5.4.1, https://meme-suite.org/tools/meme) with the parameters as follows: any number of repetitions; maximum number of motifs, 20; and, the optimum width of each motif, between 5 and 200 residues. Conserved histidine-boxes (e.g., HxxxH, HxxxH, and HxxHH) and the ER retention signal were manually checked.

Synteny analysis, duplication modes, and definition of orthogroups

Synteny analysis was conducted using TBtools-II (v2.152) as described before [41], whereas orthologous genes and different duplication modes were identified using Orthofinder (v2.3.8) [54] and the DupGen_finder pipeline [55], respectively.

Gene expression analysis based on RNA-seq

Two Illumina RNA-seq datasets, which are under NCBI accession numbers of PRJNA703731 and PRJNA671562, were first analyzed in this study. They are 150 bp paired-end reads with three biological replicates. Quality control, read mapping, and differential analysis were performed using Trimmomatic, HISAT, and DESeq2 as previously described [56–59], and relative gene expression level was presented as FPKM [60].

Plant materials and qRT-PCR analysis

Tigernut plants of the Reyan3 variety were grown as previously described [20]. For qRT-PCR analysis, five representative stages of tuber development were collected at 1, 10, 20, 25, and 35 DAI, which represent tuber initiation, three stages of swelling, and maturation as described before [40]. Samples with three biological replicates were freezed with liquid nitrogen and subjected to RNA isolation. Total RNA extraction, the integrity and concentration detection, synthesis of the first-strand cDNA, and qRT-PCR analysis were conducted as described before [24, 61]. Primers used in this study are shown in Additional file 5, where *CeTIP41* and *CeUCE2* are two reference genes. Relative gene abundance was estimated with the $2^{-\Delta\Delta Ct}$ method and statistical analysis was performed using the Data Processing System software v20, where differences among means were tested following Duncan's one-way multiple-range post hoc ANOVA.

Supplementary Information

The online version contains supplementary material available at https://doi.org/10.1186/s12870-025-06398-w.

Additional file 1. Percent similarity within and between CeFADs and AtFADs.

Additional file 2. Chromosomal localization and duplication events of *AtFAD* genes.

Additional file 3. Protein domains and motifs of CeFADs.

Additional file 4. *FAD* genes identified in representative plant species.

Additional file 5 Primers used in this study.

Acknowledgements

The authors appreciate those contributors who make the related genome and transcriptome data accessible in public databases. They also thank helpful suggestions from reviewers. It's worth noting that, as expected, a FAD4 homolog was successfully identified from leaf and sheath transcriptomes of purple nutsedge, which are available when the paper is under review.

Authors' contributions

The study was conceived and directed by ZZ. All the experiments and analyses were directed by ZZ and carried out by ZZ, XF, CL, JH, and ZY. ZZ, JH, and ZY wrote the paper. All the authors read and approved the final manuscript.

Funding

This work was supported by the Hainan Province Science and Technology Special Fund (ZDYF2024XDNY171 and ZDYF2024XDNY156), the National Natural Science Foundation of China (32460342 and 31971688), and the Project of National Key Laboratory for Tropical Crop Breeding (NKLTCB202325). The funders had no role in study design, data collection and analysis, decision to publish, or preparation of the manuscript.

Data availability

The datasets analyzed during the current study are available in the NCBI SRA repository (https://www.ncbi.nlm.nih.gov/sra/) under accession numbers of PRJNA703731 and PRJNA671562.

Declarations

Ethics approval and consent to participate

Not applicable.

Consent for publication

Not applicable.

Competing interests

The authors declare no competing interests.

Author details

[1]National Key Laboratory for Tropical Crop Breeding/Hainan Key Laboratory for Biosafety Monitoring and Molecular Breeding in Off-Season Reproduction Regions, Institute of Tropical Biosciences and Biotechnology/Sanya Research Institute of Chinese Academy of Tropical Agricultural Sciences, Haikou, Hainan 571101, P. R. China. [2]School of Breeding and Multiplication (Sanya Institute of Breeding and Multiplication) and College of Tropical Agriculture and Forestry, Hainan University, Sanya, Hainan 572025, P. R. China. [3]College of Biology and Food Engineering, Guangdong University of Petrochemical Technology, Maoming, Guangdong 525000, P. R. China.

Received: 21 January 2025 Accepted: 13 March 2025
Published online: 26 March 2025

References

1. Ohlrogge J, Browse J. Lipid biosynthesis. Plant Cell. 1995;7(7):957–70.
2. Shanklin J, Cahoon EB. Desaturation and related modifications of fatty acids. Annu Rev Plant Biol. 1998;49:611–41.
3. Kazaz S, Barthole G, Domergue F, Ettaki H, To A, Vasselon D, et al. Differential activation of partially redundant Δ9 stearoyl-ACP desaturase genes is critical for omega-9 monounsaturated fatty acid biosynthesis during seed development in Arabidopsis. Plant Cell. 2020;32(11):3613–37.
4. Heilmann I, Mekhedov S, King B, Browse J, Shanklin J. Identification of the Arabidopsis palmitoyl-monogalactosyldiacylglycerol delta7-desaturase gene FAD5, and effects of plastidial retargeting of Arabidopsis desaturases on the *fad5* mutant phenotype. Plant Physiol. 2004;136(4):4237–45.
5. Smith MA, Dauk M, Ramadan H, Yang H, Seamons LE, Haslam RP, et al. Involvement of Arabidopsis ACYL-COENZYME A DESATURASE-LIKE2 (At2g31360) in the biosynthesis of the very-long-chain monounsaturated fatty acid components of membrane lipids. Plant Physiol. 2013;161(1):81–96.
6. Gao J, Ajjawi I, Manoli A, Sawin A, Xu C, Froehlich JE, et al. FATTY ACID DESATURASE4 of Arabidopsis encodes a protein distinct from characterized fatty acid desaturases. Plant J. 2009;60(5):832–9.
7. Sperling P, Zähringer U, Heinz E. A sphingolipid desaturase from higher plants. Identification of a new cytochrome b5 fusion protein. J Biol Chem. 1998;273(44):28590–6.
8. Ternes P, Franke S, Zähringer U, Sperling P, Heinz E. Identification and characterization of a sphingolipid delta 4-desaturase family. J Biol Chem. 2002;277(28):25512–8.
9. Feng J, Dong Y, Liu W, He Q, Daud MK, Chen J, et al. Genome-wide identification of membrane-bound fatty acid desaturase genes in

Gossypium hirsutum and their expressions during abiotic stress. Sci Rep. 2017;7:45711.
10. E Z, Chen C, Yang J, Tong H, Li T, Wang L, et al. Genome-wide analysis of fatty acid desaturase genes in rice (*Oryza sativa* L.). Sci Rep. 2019;9(1):19445.
11. Xu L, Zeng W, Li J, Liu H, Yan G, Si P, et al. Characteristics of membrane-bound fatty acid desaturase (FAD) genes in *Brassica napus* L. and their expressions under different cadmium and salinity stresses. Environ Exp Bot. 2019;162:144–56.
12. Laureano G, Cavaco AR, Matos AR, Figueiredo A. Fatty acid desaturases: Uncovering their involvement in grapevine defence against downy mildew. Int J Mol Sci. 2021;22(11):5473.
13. Li J, Liu A, Najeeb U, Zhou W, Liu H, Yan G, et al. Genome-wide investigation and expression analysis of membrane-bound fatty acid desaturase genes under different biotic and abiotic stresses in sunflower (*Helianthus annuus* L.). Int J Biol Macromol. 2021;175:188–98.
14. Niu E, Gao S, Hu W, Zhang C, Liu D, Shen G, et al. Genome-wide identification and functional differentiation of fatty acid desaturase genes in *Olea europaea* L. Plants (Basel). 2022;11(11):1415.
15. Wei H, Movahedi A, Xu S, Zhang Y, Liu G, Aghaei-Dargiri S, et al. Genome-wide characterization and expression analysis of fatty acid desaturase gene family in poplar. Int J Mol Sci. 2022;23(19):11109.
16. Cao T, Du Q, Ge R, Li R. Genome-wide identification and characterization of FAD family genes in barley. PeerJ. 2024;12: e16812.
17. Ye Z, Mao D, Wang Y, Deng H, Liu X, Zhang T, et al. Comparative genome-wide identification of the fatty acid desaturase gene family in tea and oil tea. Plants (Basel). 2024;13(11):1444.
18. Govaerts R, Nic Lughadha E, Black N, Turner R, Paton A. The World Checklist of Vascular Plants, a continuously updated resource for exploring global plant diversity. Sci Data. 2021;8(1):215.
19. Zou Z, Xiao YH, Zhang L, Zhao YG. Analysis of *Lhc* family genes reveals development regulation and diurnal fluctuation expression patterns in *Cyperus esculentus*, a Cyperaceae plant. Planta. 2023;257(3):59.
20. Zou Z, Zheng YJ, Xiao YH, Liu HY, Huang JQ, Zhao YG. Molecular insights into PIP aquaporins in tigernut (*Cyperus esculentus* L.), a Cyperaceae tuber plant. Tropical Plants. 2024;3:e027.
21. Zou Z, Fu XW, Li CQ, Yi XP, Huang JQ, Zhao YG. Integrative analysis provides insights into genes encoding LEA_5 domain-containing proteins in tigernut (*Cyperus esculentus* L.). Plants. 2025;14(5):762.
22. Turesson H, Marttila S, Gustavsson KE, Hofvander P, Olsson ME, Bülow L, et al. Characterization of oil and starch accumulation in tubers of *Cyperus esculentus* var. *sativus* (Cyperaceae): A novel model system to study oil reserves in nonseed tissues. Am J Bot. 2010;97(11):1884–93.
23. Codina-Torrella I, Guamis B, Trujillo AJ. Characterization and comparison of tiger nuts (*Cyperus esculentus* L.) from different geographical origin. Ind Crop Prod. 2015;65:406–14.
24. Zou Z, Zhao YG, Zhang L, Kong H, Guo YL, Guo AP. Single-molecule real-time (SMRT)-based full-length transcriptome analysis of tigernut (*Cyperus esculentus* L.). Chin J Oil Crop Sci. 2021;43:229–35.
25. Ji HY, Liu DT, Yang ZL. High oil accumulation in tuber of yellow nutsedge compared to purple nutsedge is associated with more abundant expression of genes involved in fatty acid synthesis and triacylglycerol storage. Biotechnol Biofuels. 2021;14(1):54.
26. Yang X, Niu L, Zhang Y, Ren W, Yang C, Yang J, Xing G, et al. Morpho-agronomic and biochemical characterization of accessions of tiger nut (*Cyperus esculentus*) grown in the north temperate zone of China. Plants (Basel). 2022;11(7):923.
27. Wu ZW, Huang HR, Liao SQ, Cai XS, Liu HM, Ma YX, et al. Evaluation of quality properties of brown tigernut (*Cyperus esculentus* L.) tubers from six major growing regions of China: A new source of vegetable oil and starch. J Oleo Sci. 2024;73(2):147–61.
28. Zhang H, Zhu Z, Di Y, Luo J, Su X, Shen Y, et al. Understanding the triacylglycerol-based carbon anabolic differentiation in *Cyperus esculentus* and *Cyperus rotundus* developing tubers via transcriptomic and metabolomic approaches. BMC Plant Biol. 2024;24(1):1269.
29. Li T, Sun Y, Chen Y, Gao Y, Gao H, Liu B, et al. Characterisation of two novel genes encoding Δ9 fatty acid desaturases (CeSADs) for oleic acid accumulation in the oil-rich tuber of *Cyperus esculentus*. Plant Sci. 2022;319: 111243.
30. Zou Z, Fu XW, Li CQ, Yi XP, Huang JQ, Zhao YG. Insights into the stearoyl-acyl carrier protein desaturase (SAD) family in tigernut (*Cyperus esculentus* L.), an oil-bearing tuber plant. Plants. 2025;14(4):584.
31. Zhao X, Yi L, Ren Y, Li J, Ren W, Hou Z, et al. Chromosome-scale genome assembly of the yellow nutsedge (*Cyperus esculentus*). Genome Biol Evol. 2023;15(3):evad027.
32. Wang W, Haberer G, Gundlach H, Gläßer C, Nussbaumer T, Luo MC, et al. The *Spirodela polyrhiza* genome reveals insights into its neotenous reduction fast growth and aquatic lifestyle. Nat Commun. 2014;5:3311.
33. Olsen JL, Rouzé P, Verhelst B, Lin YC, Bayer T, Collen J, et al. The genome of the seagrass Zostera marina reveals angiosperm adaptation to the sea. Nature. 2016;530(7590):331–5.
34. Guo X, Wang F, Fang D, Lin Q, Sahu SK, Luo L, et al. The genome of *Acorus* deciphers insights into early monocot evolution. Nat Commun. 2023;14(1):3662.
35. Carey SB, Aközbek L, Lovell JT, Jenkins J, Healey AL, Shu S, et al. ZW sex chromosome structure in *Amborella trichopoda*. Nat Plants. 2024;10(12):1944–54.
36. Niemeyer PW, Irisarri I, Scholz P, Schmitt K, Valerius O, Braus GH, et al. A seed-like proteome in oil-rich tubers. Plant J. 2022;112(2):518–34.
37. Zou Z, Zhao YG, Zhang L, Xiao YH, Guo AP. Analysis of *Cyperus esculentus SMP* family genes reveals lineage-specific evolution and seed desiccation-like transcript accumulation during tuber maturation. Ind Crop Prod. 2022;187: 115382.
38. Zhao Y, Fu X, Zou Z. Insights into genes encoding LEA_1 domain-containing proteins in Cyperus esculentus, a desiccation-tolerant tuber plant. 2024;13(20):2933.
39. Jiao Y, Li J, Tang H, Paterson AH. Integrated syntenic and phylogenomic analyses reveal an ancient genome duplication in monocots. Plant Cell. 2014;26(7):2792–802.
40. Zou Z, Zheng Y, Zhang Z, Xiao Y, Xie Z, Chang L, et al. Molecular characterization of *oleosin* genes in *Cyperus esculentus*, a Cyperaceae plant producing oil in underground tubers. Plant Cell Rep. 2023;42(11):1791–808.
41. Zou Z, Zheng Y, Chang L, Zou L, Zhang L, Min Y, et al. TIP aquaporins in *Cyperus esculentus*: genome-wide identification, expression profiles, subcellular localizations, and interaction patterns. BMC Plant Biol. 2024;24(1):298.
42. Arondel V, Lemieux B, Hwang I, Gibson S, Goodman HM, Somerville CR. Map-based cloning of a gene controlling omega-3 fatty acid desaturation in Arabidopsis. Science. 1992;258(5086):1353–5.
43. Okuley J, Lightner J, Feldmann K, Yadav N, Lark E, Browse J. Arabidopsis FAD2 gene encodes the enzyme that is essential for polyunsaturated lipid synthesis. Plant Cell. 1994;6(1):147–58.
44. van de Loo FJ, Broun P, Turner S, Somerville C. An oleate 12-hydroxylase from Ricinus communis L. is a fatty acyl desaturase homolog. Proc Natl Acad Sci U S A. 1995;92(15):6743–7.
45. Bowers JE, Chapman BA, Rong J, Paterson AH. Unravelling angiosperm genome evolution by phylogenetic analysis of chromosomal duplication events. Nature. 2003;422(6930):433–8.
46. Wu W, Feng X, Wang N, Shao S, Liu M, Si F, et al. Genomic analysis of *Nypa fruticans* elucidates its intertidal adaptations and early palm evolution. J Integr Plant Biol. 2024;66(4):824–43.
47. Bredeson JV, Lyons JB, Oniyinde IO, Okereke NR, Kolade O, Nnabue I, et al. Chromosome evolution and the genetic basis of agronomically important traits in greater yam. Nat Commun. 2022;13(1):2001.
48. Wang Y, Wang X, Paterson AH. Genome and gene duplications and gene expression divergence: a view from plants. Ann N Y Acad Sci. 2012;1256:1–14.
49. Miquel M, Browse J. Arabidopsis mutants deficient in polyunsaturated fatty acid synthesis. Biochemical and genetic characterization of a plant oleoyl-phosphatidylcholine desaturase. J Biol Chem. 1992;267(3):1502–9.
50. Iba K, Gibson S, Nishiuchi T, Fuse T, Nishimura M, Arondel V, et al. A gene encoding a chloroplast omega-3 fatty acid desaturase complements alterations in fatty acid desaturation and chloroplast copy number of the fad7 mutant of *Arabidopsis thaliana*. J Biol Chem. 1993;268(32):24099–105.
51. Gibson S, Arondel V, Iba K, Somerville C. Cloning of a temperature-regulated gene encoding a chloroplast omega-3 desaturase from *Arabidopsis thaliana*. Plant Physiol. 1994;106(4):1615–21.

52. Altschul SF, Madden TL, Schaffer AA, Zhang J, Zhang Z, Miller W, et al. Gapped BLAST and PSI-BLAST: a new generation of protein database search programs. Nucleic Acids Res. 1997;25(17):3389–402.
53. Tamura K, Stecher G, Peterson D, Filipski A, Kumar S. MEGA6: Molecular Evolutionary Genetics Analysis version 6.0. Mol Biol Evol. 2013;30(12):2725–9.
54. Emms DM, Kelly S. OrthoFinder: phylogenetic orthology inference for comparative genomics. Genome Biol. 2019;20(1):238.
55. Qiao X, Li Q, Yin H, Qi K, Li L, Wang R, et al. Gene duplication and evolution in recurring polyploidization-diploidization cycles in plants. Genome Biol. 2019;20(1):38.
56. Bolger AM, Lohse M, Usadel B. Trimmomatic: a flexible trimmer for Illumina sequence data. Bioinformatics. 2014;30(15):2114–20.
57. Kim D, Langmead B, Salzberg SL. HISAT: a fast spliced aligner with low memory requirements. Nat Methods. 2015;12(4):357–60.
58. Love MI, Huber W, Anders S. Moderated estimation of fold change and dispersion for RNA-seq data with DESeq2. Genome Biol. 2014;15(12):550.
59. Zou Z, Yang JH, Zhang XC. Insights into genes encoding respiratory burst oxidase homologs (RBOHs) in rubber tree (*Hevea brasiliensis* Muell. Arg.) Ind Crop Prod. 2019;128:126–39.
60. Mortazavi A, Williams BA, McCue K, Schaeffer L, Wold B. Mapping and quantifying mammalian transcriptomes by RNA-seq. Nat Methods. 2008;5(7):621–8.
61. Zou Z, Gong J, An F, Xie GS, Wang JK, Mo YY, et al. Genome-wide identification of rubber tree (*Hevea brasiliensis* Muell. Arg.) Aquaporin genes and their response to ethephon stimulation in the laticifer, a rubber-producing tissue. BMC Genomics. 2015;16:1001.

Publisher's Note